AA7xxx alloy in order to reduce the grain size of with addition of AA7xxx+0.5% SC; Study their Microstructure, Mechanical properties,Thermal properties and Stress Corrosion cracking behaviour

Siyyadri Adinarayana
Department of Mechanical Engineering, N S Raju Institute of Technology (NSRIT) Autonomous, Visakhapatnam, A.P, India

P. N. E. Naveen
Department of Mechanical Engineering, N S Raju Institute of Technology (NSRIT) Autonomous, Visakhapatnam, A.P, India

V.V. Ravi Kumar
Department of Mechanical Engineering, N S Raju Institute of Technology (NSRIT) Autonomous, Visakhapatnam, A.P, India

K. Ram Prasad
Department of Mechanical Engineering, N S Raju Institute of Technology (NSRIT) Autonomous, Visakhapatnam, A.P, India

Abstract
Purpose- In order to reduce the grain size with addition AA-7xxx+Sc alloy, study their mechanical properties, microstructure and corrosion behaviour of AA-7xxx with AA-7xxx + wt% (0.5Sc) alloys. Precipitation hardening of above conditions was investigated.
Design/methodology/approach- Precipitates at different age-hardening conditions were measured of nano scale precipitates $MgZn_2$, Al_2Cu and Al_3Sc. The precipitation hardening behaviour of AA-7xxx+0.5 wt.% Sc alloys are studied on the basis of optical microscopy, electron microscopy (SEM & TEM), XRD observations, mechanical properties and electrochemical analysis.
Findings- AA 7xxx and AA-7xxx+0.5 wt.% Sc alloys were developed casting method and comparing mechanical properties, microstructure and stress corrosion cracking behaviour ofusing 3% NaCl solution medium to understand the corrosion behaviour of alloy such as AA 7xxx and AA-7xxx+0.5 wt.% Sc ally , AA-7xxx+0.5 wt.% Sc precipitation hardened (T6) alloy.
Originality/value- Hardness, mechanical properties and Stress corrosion cracking behaviour of AA-7xxx with AA-7xxx + wt% (0.5Sc) alloys and understand the corrosion behaviour of alloy such as AA 7xxx and AA-7xxx+0.5 wt.% Sc ally , AA-7xxx+0.5 wt.% Sc precipitation hardened (T6) alloy and potentio-dynamic polarization (PDP) curves.

Keywords: AA7xxx alloys, Stress corrosion cracking, Precipitation hardening, Transmission electron microscopy (TEM), AA-7XXX+0.5%Sc.

Introduction

Aluminium alloys are prominent materials like aerospace, marine, naval and auto mobile applications. Ultra-fine grained (UFG) materials possess superior mechanical properties which have attracted the scientific community in the past few decades. These structured materials offer a significant improvement in strength without compromising ductility and toughness. In specific, AA7xxx series alloys are most recommended light weight aluminium alloy for aerospace applications due to their high specific strength, resistance to various corrosive media, etc. Proper selection of alloying additions and thermo- mechanical processing will be considered as key strengthening factors which facilitate the formation of the desirable compounds and refining

grain size. Increasing alloying additions in AA7xxx series resulted in formation of complex intermetallic compounds, either soluble or insoluble compounds [1–4]. Scandium is the most effective precipitation hardener element in Al alloys. Al-Sc alloys have excellent mechanical properties at ambient and elevated temperatures due to the presence of a high number density of elastically hard Al_3Sc precipitates [5-6]. The high response to precipitation hardening mechanisms is a homogeneous dispersion of Al_3Sc particles, formed during solid solution strengthening and grain boundaries strengthening mechanisms [7-8]. Galvanic corrosion and pitting corrosion are common in aircraft structure in particular, marine environments [9]. However, Al-Zn-Mg alloys are susceptible to various forms of localized corrosion such as pitting and intergranular corrosion (IGC) and stress corrosion cracking in chloride environment,.[10-12]. Precipitates at the grain boundaries further results in the formation of precipitates-free zones along the grain boundaries. These precipitates-free zones result in localized attack along the grain boundary, leading to IGC. The size and distribution of deleterious particles, strengthening precipitates are influenced by precipitation hardening treatment [13-17]. Differentiated with some other high-strength aluminium alloys, the alloy exhibited better corrosion resistance was higher than some AA 8xxx aluminium alloys [18-20]. The present study the effect of Sc addition on the microstructure of as cast Al-Sc alloys and the precipitation hardening response of with solution heat treatment and effect of the corrosion in aluminium alloys with 3%Nacl behaviour.

Literature Review

Aluminum alloys are the potential candidate materials for aircraft structures due to their high strength to weight ratio, corrosion resistance, machinability, low cost etc. Aluminium alloys with secondary phases are susceptible to corrosion which is anodic in comparison to the matrix [Andreatta et al. (2018); Yang et al. (2019)]. There are other factors which contribute corrosion in aircraft structures such as humidity, rain, temperature and salt water. Galvanic corrosion and pitting corrosion are common in aircraft structure in particular, marine environments [Mario and Vinod (2011)]. Improvement in strength along with improved corrosion resistance for marine environment is beneficial for marine applications. However, Al-Zn-Mg alloys are susceptible to various forms of localized corrosion such as pitting, crevice, intergranular corrosion (IGC) and stress corrosion cracking in chloride environment. In addition to chemical composition, microstructure is considered to be a critical factor in deciding the corrosion behaviour of metallic materials [Meng et al. (2016); Pantelakis et al. (2000)].

Experimental procedures

Material selection and X-ray diffraction (XRD) analysis

AA7xxx aluminium alloy round billet was fabricated by casting method, chemical composition of AA 7xxx alloy with 0.5% Sc shown in Table-1. The sizes of the die were 350mm x 50mm. In order to understand the hardening (T6) behaviour, the alloy was solutionized at 450°C for 2 hrs. Ageing treatment was done at 120°C with different time interval. Microstructural analysis was carried out on cast alloy and Aged alloy using optical microscopy and electron microscopy (SEM & TEM). Mechanical properties such as hardness and tensile studies were

conducted on cast and precipitation hardened alloy. Tensile and hardness tests were conducted using Tinius Olsen, UK (Model: H50 KS) tensile machine and Wilson hardness, respectively. AA7xxx, AA7xxx+(0.5%)Sc, solutionized and aged alloy was evaluated by using 3% NaCl solution as corrosion medium to understand the corrosion behaviour of alloy. Surface morphology of the corroded sample was evaluated with the help of scanning electron microscopy. The susceptibility to corrosion and errosion were tested using Galvano potionstat apparatus (Make: Biologic, SP150) and subsequently corrosion rate and mass were calculated as per standards.

Table I Chemical composition AA 7xxx + (0.5%) Sc

Material	Zn	Cu	Mg	Sc	Al
Weight (%)	5-6	1-2	3-4	0.5	balance

Results and discussion

Microstructural Characterization

Micrographs of AA7xxx alloy AA7xxx with 0.5%Sc aluminium alloy various conditions shown in fig. 1(a & b). The microstructure of AA7xxx with Scandium shows α-Al matrix and complex intermetallic compounds. The grain size of cast alloy is the range of 20- 30µm. After addition of the 0.5 wt (%) scandium grain size range of 5-10µm. The complex intermetallic compounds are predominantly Al_6CuMg_4, Al_2Cu and $MgZn_2$ and Al_2CuMg by non-equilibrium solidification addition of 0.5 wt (%), Scandium form dispersoids Al_3Sc shown in XRD pattern of Fig. 2. Microstructures of solutionized and aged AA7xxx+0.5%SC alloy are shown in fig. 1(c & d). The structure of aged alloy shows dispersoids and fine precipitates. During solutionizing treatment, the chemical composition of matrix grains is getting changed. The grains of solutionized alloy are rich with Cu and Zn than that of grains of cast alloy.

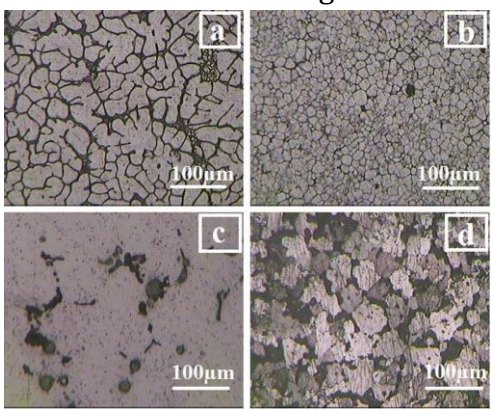

Fig . 1 Microstructure of AA 7xxx alloy at different conditions a) AA 7xxx, b) AA 7xxx + (0.5%) Sc with c) Solutionized (450˚C-2hrs) and d) Aged at 120˚C for 20hrs.

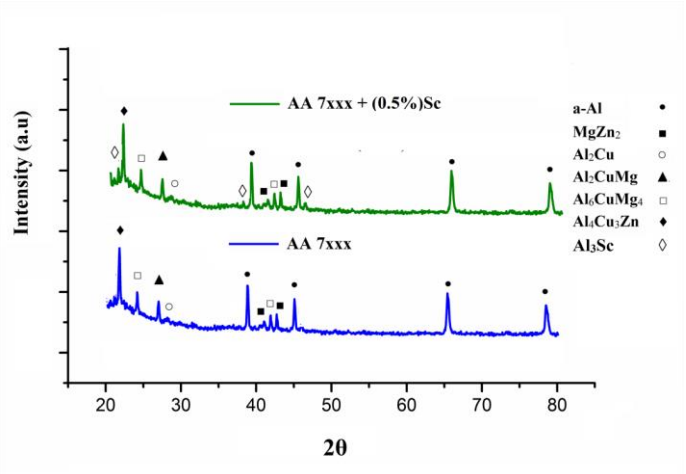

Fig. 2 X-ray diffraction patterns of AA 7xxx alloy in different conditions.

Figure 3 shows the TEM micrographs of AA7xxx alloy (aged at 120°C). Fig. 3a bright field micrograph shows fine nano size precipitates and compounds distributed uniformly in the aluminium matrix. Dark field TEM micrograph shown in fig. 3b, the reduction of the size and the distribution of inter metallic compounds are attributed to the precipitation hardening and precipitation strengthing form of Al2Cu and MgZn2 precipitates conform that evidence of SAED pattern shown in fig. 3c observed precipitates and intermetallic particles.

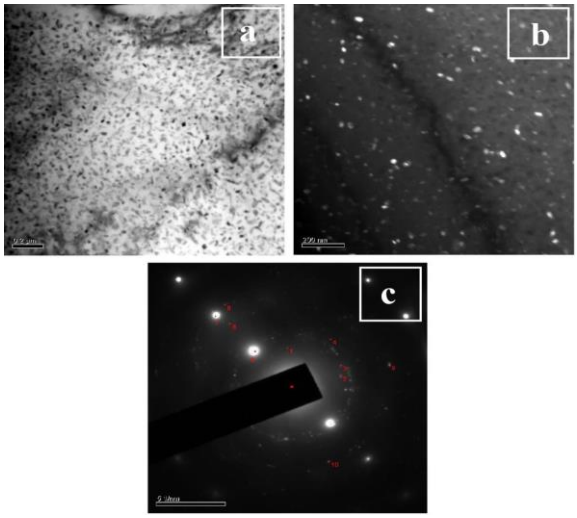

Fig. 3 TEM micrographs of AA 7xxx alloy at different conditions Aged at 120˚C for 24hrs

Figure 4 shows the TEM micrographs of AA7xxx + 0.5%Sc alloy (Aged at 120°C- 24hrs). Nano-size compounds are seen in the micrographs. T6 treated aluminium alloy AA7xxx + 0.5%Sc exhibits very nano size inter metallic compounds distributed in throught the matrix. It is observed that there are two different types of nano-size compounds such as MgZn2 and Al2Cu. TEM images of alloy exhibit fine compounds and intermetallic compounds Scandium alloy reveal fine size dispersoids like Al3Sc and grains with severe structural defects. Precipitation

hardening and dispersion strengthing form of Al_3Sc dark field TEM micrograph as shown in fig. 4b. SAED pattern of AA 7xxx alloy with 0.5%Sc alloy show soluble and insoluble intermetallic compounds observed in Fig. 4c. Precipitation behaviour of AA7xxx + 05%Sc wt. (%) alloy is a bit sluggish due to the presence of insoluble intermetallic compounds which delay the solutionizing of soluble compounds and evolution of fine precipitates during ageing. It is interesting to note that there is a precipitate free zone around the insoluble coarse intermetallic compounds, attributed by restricted atom diffusion around insoluble compound

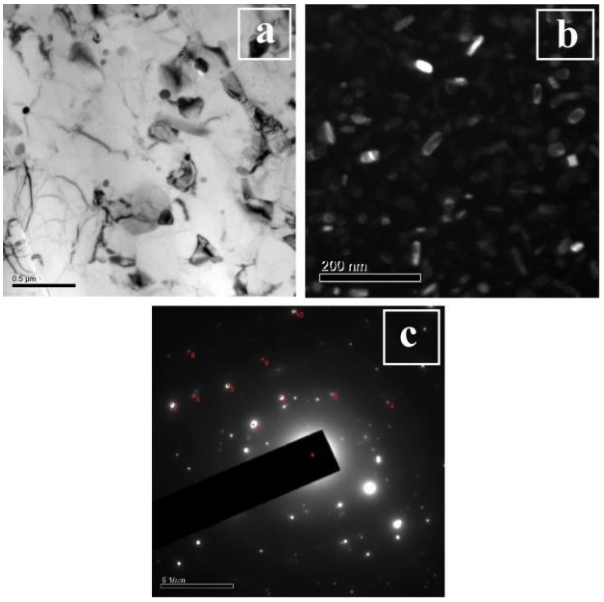

Fig. 4 TEM micrographs of AA 7xxx + 0.5%Sc alloy at different conditions Aged at 120˚Cfor 24hrs.

Mechanical properties

Precipitation hardening behaviour of AA7xxx with 0.5%Sc alloy micro Vickers hardness values of the alloy with different processes are given in Table 2. The hardness values of cast and solutionized conditions are 171±5$Hv_{0.3}$, 188±5$Hv_{0.3}$, 114±3$Hv_{0.3}$ and 136±3$Hv_{0.3}$ respectively. Solutionized alloy results shows lower hardness than that of cast alloy, which is due to dissolution harder precipitates in the matrix. The undissolved precipitates such as Al_6CuMg_4 and Al_2CuMg are coarser in size and their contribution is minimal in enhancing hardness. The peak hardness is obtained at different ageing temperature, 198±4$Hv_{0.3}$ for 20hrs and 212±5$Hv_{0.3}$ for 16hrs at 120°C and 160°C, respectively. After attaining peak hardness, the hardness is getting reduced by over-ageing. The peak hardness values of aged alloy are much higher than conventional AA7xxx and AA7xxx with 0.5%Sc alloy.

Table 2. Hardness values of AA7xxx with 0.5%Sc alloy with different conditions

Conditions	Hardness Values (Hv)
As Cast	171 ± 5
As Cast + 0.5%SC	188 ± 5

Solutionized(Ascast) (450°C +2hrs)	114 ± 3			
Solutionized(0.5%SC) (450°C +2hrs)	136 ± 3			
Ageing Time (hrs)	Hardness Values (Hv)			
	As Cast		As Cast + 0.5% SC	
	120°C	160°C	120°C	160°C
4	118 ±5	121±5	126±5	145±5
8	132±5	154±5	140±5	173±5
12	150±5	183±5	165±5	186±5
16	168±5	191±5	189±5	198±5
20	176±5	193±5	198±5	212±5
24	185±5	199±5	210±5	221±5
28	172±5	176±5	207±5	215±5

Mechanical properties of AA7xxx and AA7xxx with 0.5 % SC alloy with different conditions are shown in Table 3. The tensile strength of AA7xxx and AA7xxx with 0.5% Sc cast, solutionized and aged alloy is 424MPa, 480MPa, 359MPa, 642MPa and 637MPa and the elongation is 3%, 2%, 8%, 6.5% and 7.6 %, respectively. AA7xxx and AA7xxx with 0.5% Sc alloys has resulted good strength by non-homogenous nature and poor ductility of cast alloys. Age hardened aluminium alloy exhibits enhanced mechanical properties than that of cast alloy and solutionized alloy with 8% ductility. A good combination strength and ductility in bulk nano-structured AA7xxx with 0.5% SC alloy had been developed by introducing very fine secondary phase particles in the matrix. Enhancement of strength and ductility in alloy was attributed to an accumulation of dislocations, resistance to dislocation- slip by compounds, solid solution, precipitation hardening and dispersion hardening shown in fig 5. Precipitation hardening has resulted increment in UTS than that of cast alloy with good incremental ductility. This is attributed by nano-scale size of precipitates distributed homogeneously throughout the matrix addition of AA7xxx + 0.5%Sc alloy.

Table 3.Mechanical properties of AA7xxx alloy with different conditions

S.No	Conditions	(Hv0.3)	d strength (MPa)	UTS (MPa)	% Elongation
1	Cast	171±5	358±10	424±10	3.0±1
2	Cast + Sc (0.5%)	188±5	432±10	480±10	2.0±1
3	Solutionized + Sc (0.5%)	150±5	272±10	359±10	8.0±2
4	Aged + Sc (0.5%) + 120°C	205±5	525±10	642±10	6.4±2
5	Aged + Sc (0.5%) + 160°C	218±5	515±10	637±10	7.6±2

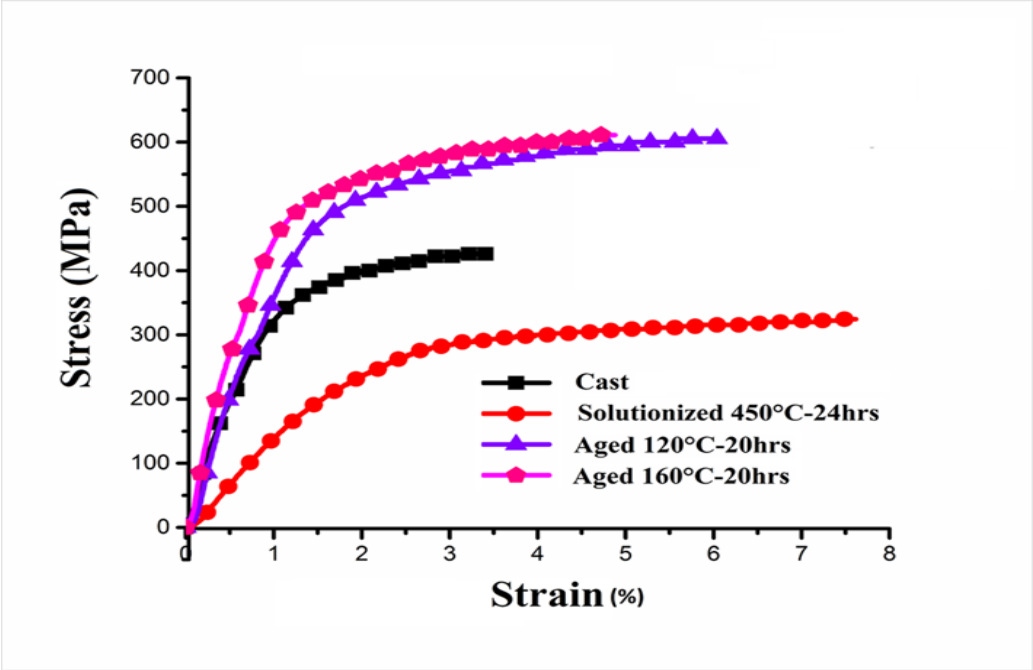

Fig 5. Stress-strain curves of AA 7xxx and AA 7xxx + 0.5% SC alloy at different conditions

The strength and hardness of aged alloy are better than that of cast and solutionized alloy. During solutionizing and quenching of AA 7xxx and AA 7xxx + 0.5% SC alloy, the solute atoms are getting dissolved. The temperature mainly acts as a driving force for transformation of supersaturated solution to stable coherent precipitates. θ' ($MgZn_2$) and θ' ($CuAl_2$) are precipitated during ageing process and it can significantly improve the strength of the aged alloy by producing obstacle for dislocation movement. The effect of ageing temperature on structural transformation and increasing mechanical properties are not appreciated due to the strong pinning effect of insoluble compounds.

Coefficient of thermal expansion

The results of coefficient of thermal expansion obtained from AA7xxx and AA 7xxx + 0.5% SC alloy with the varying Al_3SC content and in the temperature range from 30 to 250°C are shown in Fig. 6 (a). It is observed that with increase in Form Al_3SC dispersoids the CTE of AA7075 tends to decrease as expected. In all the cases composites showed a lower CTE when compared to that of unreinforced AA7xxx + 0.5 %SC alloy. Both the reinforcement's are ceramic in nature with low CTE values. When incorporated into the AA7xxx + 0.5%SC alloy matrix, they are expected to reduce the CTE of resulting hybrid composite. This is what evident from the CTE values of AA7xxx and AA 7xxx + 0.5% SC alloy which reduced. In addition to this the restriction of AA7xxx + 0.5% SC on the expansion behaviour of AA7xxx matrix is much stronger in hybrid composites than that of composites with single reinforcement. The aluminium alloys and composite have very high CTE and they expand greatly under the influence of increasing

temperature. This is of serious concern on the dimensional stability and cannot be suited for electronic packaging applications. Undoubtedly, combining multiple reinforcements with AA7xxx matrix will allows one to tailor the CTE of hybrid composites for required applications. Fig. 7 (a)–(b) shows the dimension change-temperature curves for AA7xxx matrix and composites. It can be seen from Fig. 7 (a) the cycle curve of the unreinforced AA7xxx is not close. This indicates that alloy had certain contraction at the end of each cycle. In case of AA7xxx and AA 7xxx + 0.5% SC composites it is observed that the curves are almost close which shows that there was no visible change in the dimension (Fig. 7 (b)). The thermograms shown in Fig. 4.6 correspond to one trial for each sample. Five such trials were taken for each sample and average of them. Thus it can concluded that the hybrid composites are dimensionally stable than that of unreinforced AA AA7xxx and AA 7xxx + 0.5% SC alloy when the temperature changes. The CTE of hybrid composites is affected by many factors which includes, CTE mismatch between reinforcements and AA7xxx and AA 7xxx + 0.5% SC matrix, particle size and interfacial reactions. This tensile stress generated is mainly because of CTE mismatch between the matrix and reinforcements. However during first heating stage, relaxation of tensile stress take place subsequently a begins to build up in the AA7xxx and AA 7xxx + 0.5% SC matrix. This competition between tensile stress and compressive stress results in the CTE remains unchanged at 150–250 °C for all the AA7xxx + 0.5%SC. Thermal conductivity Fig. 8 shows the thermal conductivity values for AA7xxx and AA 7xxx + 0.5% SC and composites at different form of Al3SC weight fraction and recorded at different temperatures. It is observed that the thermal conductivity of composites were lower than that of unreinforced AA7xxx. It is generally accepted that the thermal conductivity of composites largely depends upon the thermal conductivity of reinforcing materials, type of processing, microstructure and the nature of bonding between the matrix and reinforcements. In the present case both the reinforcements have very low conductivity values. Secondly the processing condition also decides the effect of consolidation on the density of composites. Though the composites formed are having uniform dispersion and good bonding of reinforcements with the matrix but the microstructure also plays an important role. The dislocations generated around the reinforcements in the AA7xxx and AA 7xxx + 0.5% SC matrix due to thermal mismatch can cause electrons and phonons scattering at the reinforcement-matrix interface. Here both the electrons and phonons are accountable for better thermal conductivity of a material. For effective conductivity the energy transfer is essential between the electrons and phonons at the interface. With increasing Al3SC dispersoids content, the increase in the dislocation density is also expected. So these dislocation causes scattering of electrons and phonons on the elastic strain field of the dislocation lines. The above mentioned does contribute significantly in the reduction of thermal conductivity values of AA 7xxx and AA7xxx + 0.5% SC composites.

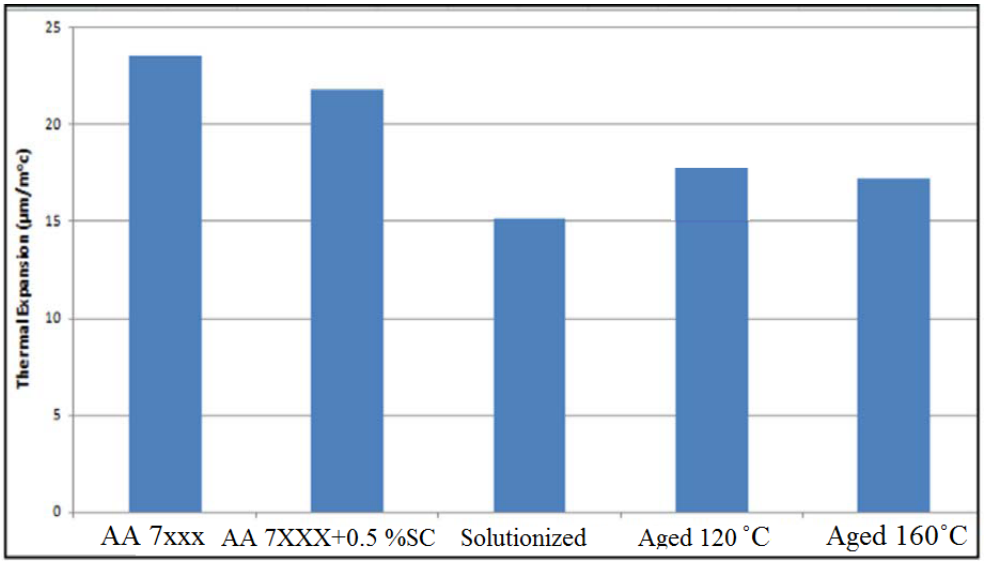

Fig. 6. Coefficient of thermal expansion of AA7xxx alloy and hybrid composites at room temperature with varying weight fractions.

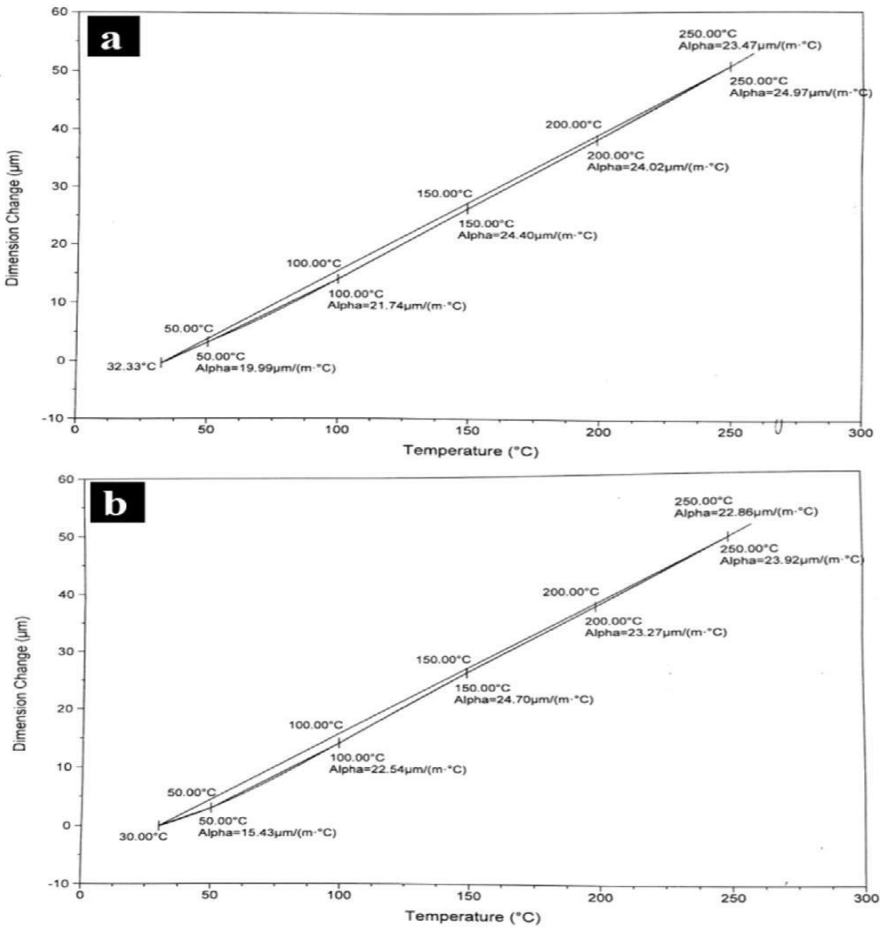

Fig. 7 Coefficient of thermal expansion curves for (a) AA7xxx, (b) AA7xxx + 0.5 % SC in various conditions.

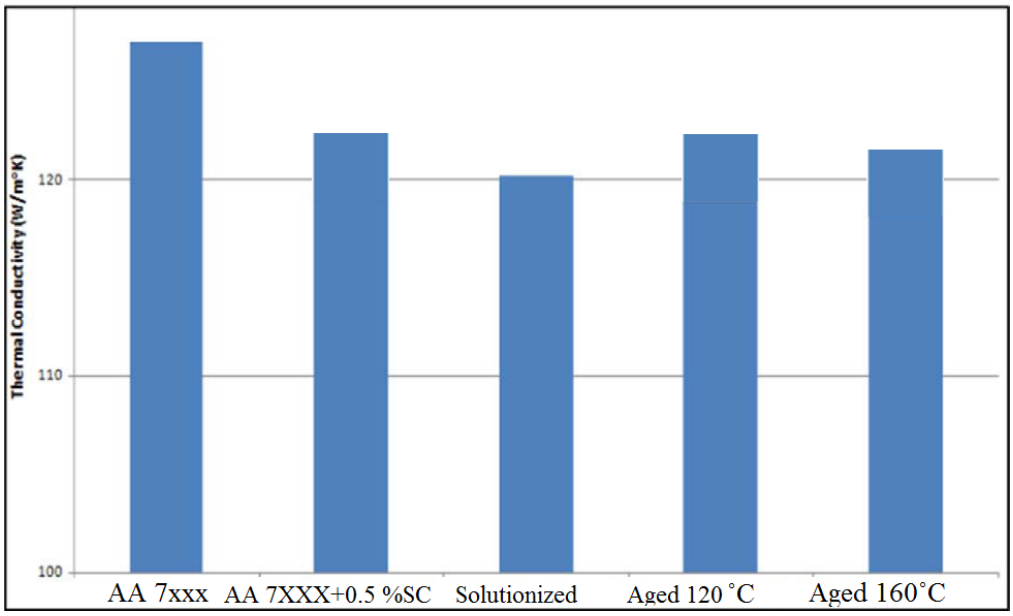

Fig. 8 Thermal conductivity of AA7xxx alloy and AA 7xxx + 0.5% SC alloy atroom temperature.

Stress corrosion cracking behavior of precipitation hardened (T6) AA 7xxx alloy

Figure 9 shows the photographs of SCC tested AA 7xxx + 0.5 % SC alloy in different processing conditions. Cast aluminium alloy SCC tested in 3.5wt. % NaCl solution with stress of 286MPa is failed at 642 hrs (26 days). The solutionized alloy is failed at 190hrs withstress of 188MPa in the same medium respectively (Table - 4). After solution treatment, the matrix chemistry has been altered with dissolved compounds. The solutionised alloy also possesses stress generated during quenching of the alloy. The combination of altered chemistry and quenched stress makes the solutionised alloy more prone to SCC at shorter interval (196hrs). T6 treated AA 7xxx + 0.5 % SC alloy (Aged 120˚C-20hrs and 160˚C- 20hrs)) gain favorable resistant to SCC. The aged alloys shows better resistant to SCC beyond 30 days as per standard. The reported SCC mechanisms are active path dissolution, hydrogen-assisted cracking and dislocation-assisted cracking. The dissolution rate of grain- boundary precipitates decides the crack velocity. Aged alloy consists of nano / ultra-fine size and coarse compounds in the matrix. The dissolution rate is decreased during SCC when the presence of larger size grain boundary particles, which, in turn, slow down the crack propagation.

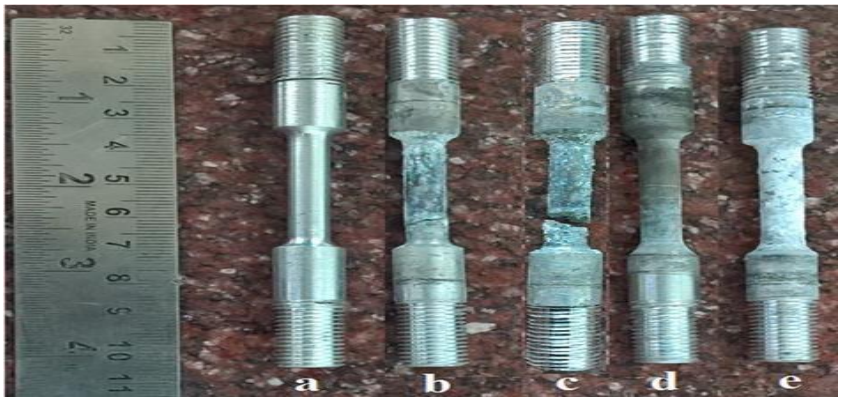

Fig 9 Photographs of SCC test on different AA 7xxx + 0.5 % SC alloy a) Cast b) Cast afterSCC c) Solutionized (450˚C-24hrs) after SCC d) Aged (120˚C-20hrs) after SCC and e) Aged (160˚C-20hrs) after SCC.

Table 4. Constant applied tensile load (CL) stress corrosion cracking tests data ofAA 7xxx and AA 7xxx + 0.5% SC alloy at different conditions

Conditions	Yield strength (MPa)	(80%) Yield strength (MPa)	Deflection	of failure(hrs)
Cast + 0.5 % SC	358±10	286	0.2	642
Solutionized- (450˚C-24hrs)	236±10	188	0.2	190
Aged-(120˚C-20hrs)	462±10	369	0.2	(failure did not occur during the maximum test period of 30 days)
Aged-(160˚C-20hrs)	485±10	388	0.2	(failure did not occur during the maximum test period of 30 days)

Fracture surface of the SCC tested AA 7xxx + 0.5 % SC alloy alloy (cast and solutionised) is shown in Fig. 10. Severe damage is noticed in the fracture surface. Combinations of brittle intergranular fracture with cleavage-like fractures are observed on the fracture surfaces of the cast alloy. Cracks are developed and propagating inwards along the grain boundaries. The synergetic effect of stress and corrosive environment with developed cracks make the alloy more susceptible to failure. This is more severe in solutionised alloy. Fracture surface is completely crumpled. The fracture surface appears like wormy morphology.

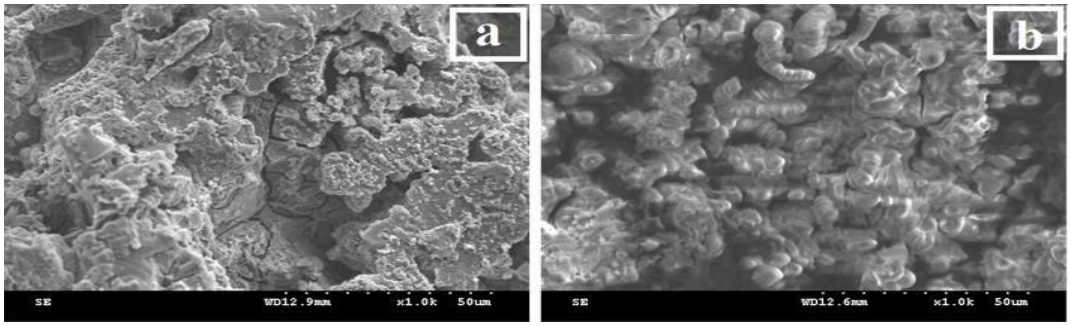

Fig 10 Constant applied tensile load (CL) stress corrosion cracking fracture surface of Al-12Zn-3Mg-2.5Cu alloy + 0.5 % SC, a) Cast and b) Solutionized (450˚C-24hrs)

Figure 11 shows the surface of SCC tested alloy in different conditions. Alloys in all conditions show the surface cracks. The severity of cracks is getting varied upon conditions. Cast and solutionised alloy show more deep cracks and it is also seen rupturing/coalesce of cracks in some localized region. EDS analysis conveys the formation of brittle oxide, in specific, Al_2O_3 which is damaged in NaCl environment under stressed condition.

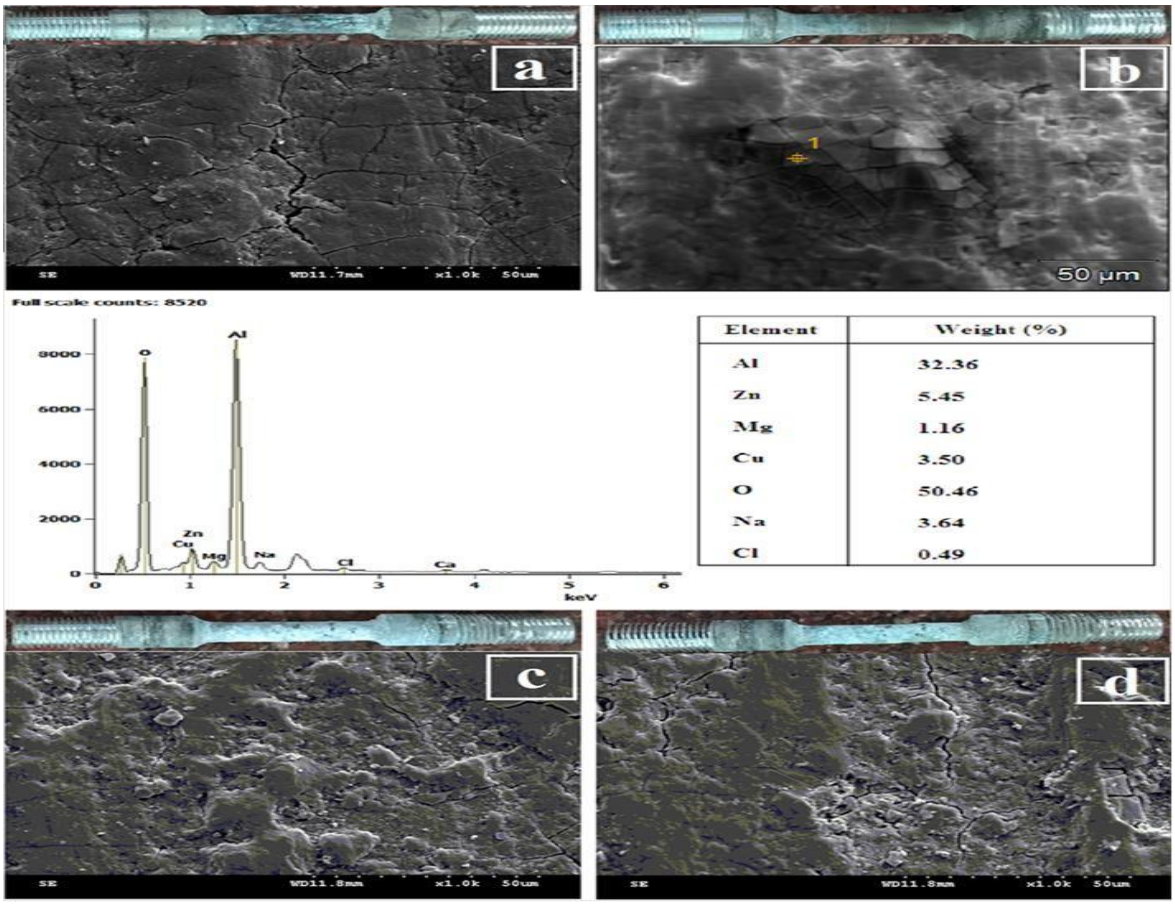

Fig 11 Constant applied tensile load (CL) stress corrosion cracking surface of AA 7xxx + 0.5% SC alloy a) Cast, b) Solutionized (450˚C-24hrs) with EDAX, c) Aged (120˚C-20hrs) conditions and d) Aged (160˚C-20hrs) condition.

Conclusions

Microstructures of AA 7xxx and AA 7xxx + 0.5% SC alloy have been tailored by adopting thermal treatment and thermo-mechanical processing for enhancing mechanical properties

- Cast AA 7xxx, wt.% alloy shows coarse intermetallic compound, both soluble and insoluble, homogeneously distributed throughout the matrix and grain boundaries

- Precipitation behaviour of AA 7xxx and AA 7xxx + 0.5% SC alloy is a bit sluggish dueto the presence of insoluble intermetallic compounds which delay the solutionizing of soluble compounds and evolution of fine precipitates during ageing. It is interesting to note that there is a precipitate free zone around the insoluble coarse intermetallic compounds, attributed by restricted atom diffusion around insoluble compound.

- Precipitation hardening has resulted 40% increment in UTS than that of cast alloy with 6% ductility. This is attributed by nano-scale size of precipitates distributed homogeneously throughout the matrix

- The CTE of developed hybrid composites decreased with the increasing TiO2 content displaying better dimensional stability. However the thermal conductivity was not improved mainly because of low thermal conductivity values of reinforcements and absence of efficient electron-phonon coupling due to scattering of the electrons and phonons at the interface

- Corrosion mechanism is predominantly galvanic in nature. The severity of galvanic behaviour is dependent on structural features such as composition of the matrix grains, grain size, secondary compounds and their size & distribution, structural homogeneity, structural defects, etc

- The alloy with the combination all the above severely degrade the materials in prescribed NaCl solution. Solutionized and aged alloy have offered good corrosion resistance than that of other processing conditions

Precipitation hardened alloy (T6 condition)) exhibits better stress corrosion resistant than that of cast and solutionised alloy. This is attributed with uniform distribution of fine precipitate in the grain and grain-boundary

Acknowledgement

My sincere thanks to Sai Surface Coating Technologies, Pashamylaram, Hyderabad to support us in facilitating the coatings.

Conflicts of interest

The authors have no conflicts of interest to declare.

Author's Contribution Statement

P N E Naveen: Conceptualization, formal analysis, methodology, validation and writing draft. **V.V. Ravi Kumar:** Conceptualization, formal analysis, methodology. **Siyyadri Adinarayana:** Conceptualization, experimentation, formal analysis and methodology

References

[1]. M. Dixit, R.S. Mishra, K.K. Sankaran, 2008. Structure–property correlations in Al 7050 and Al 7055 high-strength aluminium alloys. Materials Science and Engineering A, 478: 163–172.

[2]. Tolga Dursun, Costas Soutis, 2014. Recent developments in advanced aircraft aluminium alloys. Materials and Design, 56: 862–871.

[3]. MohammadAlipour, BaharakGhorbanian Aghdam, HamidEbrahimi Rahnoma, M. Emamya, 2013. Investigation of the effect of Al–5Ti–1B grain refiner on dry sliding wear behaviorof an Al–Zn–Mg–Cu alloy formed by strain-induced melt activation process. Materials and Design, 46: 766–775.

[4]. A.Abolhasani, A.Zarei-Hanzaki, H.R.Abedi, M.R.Rokni, 2012. The room temperature mechanical properties of hot rolled 7075 aluminium alloy. Materials and Design, 34: pp. 631–636.

[5]. Thomas Dorin, Mahendra Ramajayam, Alireza Vahid, Timothy Langan, 2018. Aluminium Scandium Alloys. Fundamentals of Aluminium Metallurgy. https://doi.org/10.1016/B978-0-08-102063-0.00012-6.

[6]. Julien Kovac, Heinz-Rolf Stock, Bernd Köhler, Hubert Bomas, Hans-Werner Zoch (2013). Tensile properties of magnetron sputtered aluminum scandium and aluminum zirconium thin films: A comparative study. Surface & Coatings Technology 215 (2013) 369-375.

[7]. Stefan Mertina, Bernd Heinzb, Oliver Rattundeb, Gabriel Christmannc, Marc- Alexandre Duboisc, Sylvain Nicolayc, Paul Muralta, 2018. Piezoelectric and structural properties of c-axis textured aluminium, scandium nitride thin films up to high scandium content. Surface & Coatings Technology 343 (2018) 2–6.

[8]. S. Vigneshwaran, K. Sivaprasadb, R. Narayanasamya, K. Venkateswarlu, (2018). Formability and Fracture Behaviour of Cryorolled Al-3Mg-0.25 Sc Alloy. Materials Science & Engineering A. doi.org/10.1016/j.msea.2018.02.072.

[9] Mario colavita, Vinod agarwala.Galvanic sensor for monitoring structural damage. Nato Otan, RTO-MP-AVT-144, (27): 1-10

[10] Chunyan Meng, Di Zhang, Cui Hua, Linzhong Zhuang, Jishan Zhang. Mechanical properties, intergranular corrosion behavior. Journal of Alloys and Compounds 617

(2014) 925–932. and microstructure of Zn modified Al–Mg alloys.

[11] Sp.G. Pantelakis, P.G. Daglaras, Ch.Alk. Apostolopoulos. Tensile and energy density properties of 2024, 6013, 8090 and 2091 aircraft aluminum alloy after corrosion exposure. Theoretical and Applied Fracture Mechanics 33 (2000) 117-134.

[12] Xing Huang, Qinglin Pan, Bo Li, Zhiming Liu, Zhiqi Huang, Zhimin Yin. Microstructure, mechanical properties and stress corrosion cracking of Al-Zn-Mg-Zr alloy sheet with trace amount of Sc. Journal of Alloys and Compounds 650 (2015) 805-820.

[13] Chunyan Meng, Di Zhang, Linzhong Zhuang, Jishan Zhang. Correlations between stress corrosion cracking, grain boundary precipitates and Zn content of Al-Mg-Zn alloys. Journal of Alloys and Compounds 655 (2016) 178-187.

[14] K.Sivaprasad, V.Swarnalatha, V.V.Ravikumar, V.Muthupandi. Influence of short annealing treatment on corrosion behaviour of cryorolled commercially pure aluminum. Anti-Corrosion Methods and Materials 57(2010) 18-20.

[15] V.V.Ravikumar and S.Kumaran. Microstructure and corrosion behaviour of precipitation hardened and thermo-mechanical treated high strength Al-12Zn-3Mg-2.5Cu alloy. Anti-Corrosion Methods and materials,65(2017):DOI10.1108/ACMM-04-2017-1780.

[16] A. Boag, A.E. Hughes, A.M. Glenn, T.H. Muster, D. McCulloch. Corrosion of AA2024-T3 Part I: Localised corrosion of isolated IM particles. Corrosion Science 53 (2011) 17–26.

[17] Xiao Yan Liu, Meng Jie Li, Fei Gao, Shun Xing Liang, Xi Liang Zhang, Hao Xuan Cui. Effects of aging treatment on the intergranular corrosion behavior of Al–Cu–Mg– Ag alloy. Journal of Alloys and Compounds 639 (2015) 263–267.

[18] Kun Zhou, Bin Wang, Yu Zhao, Jie Liu. Corrosion and electrochemical behaviors of 7A09 Al–Zn–Mg–Cu alloy in chloride aqueous solution. Trans. Nonferrous Met.Soc. China 25(2015) 2509–2515.

[19] Joachim Wloka, Sannakaisa Virtanen. Microstructural Effects on the Corrosion Behavior of High-Strength Al–Zn–Mg–Cu Alloys in an Over aged Condition. Journal of The Electrochemical Society, 154 (2007) C411-C423.

[20] Pantelakis Sp.G, P.G. Daglaras and Ch. Apostolopoulos (2000). Tensile and energy density properties of 2024, 6013, 8090 and 2091 aircraft aluminum alloy after corrosion exposure. Applied Fracture Mechanics, 33: 117-134

[21] . Oleiwi, Jawad K., Sihama I. Salih, And Hwazen S. Fadhil. "Water Absorption And Thermal Properties Of Pmma Reinforced By Natural Fibers For Denture Applications." *International Journal Of Mechanical And Production Engineering Research And Development* 8.3 (2018): 1105-1116.

[22] Saakashvili, G., M. Mohan, And E. Goud. "Mechanical Characteristics Of Ceramic Particulate Reinforced Al7075 Metal Matrix Composites And Effect Of Age Hardening On Its Tensile Properties." *International Journal Of Mechanical And Production Engineering Research And Development* 8 (2018): 173-180.

[23] Satyanarayana, K. R., B. Surendra Babu, And B. Ramesh Chandra. "Microstructurural Characterization Of 6063 Aluminium Alloy Nano-Composites." *International Journal Of Mechanical And Production Engineering Research And Development* 8.2 (2018): 851-856.

[24] El-Shennawy, M., Et Al. "Effect Of Boron Content On Metallurgical And Mechanical Characteristics Of Low Carbon Steel." *International Journal Of Mechanical Engineering* 5.2

(2016): 2319-2259.

[25] Saber, D., Kh Abd El-Aziz, And A. Fathy. "Corrosion Behavior Of Copper–Alumina Nanocomposites In Different Corrosive Media." *Int. J. Mech. Eng* 5 (2016): 1-10.

[26] El-Shennawy, M., Adel A. Omar, And M. Ayad. "Similar And Dissimilar Friction Stir Welding Of Aa7075." *International Journal Of Mechanical Engineering (Ijme)* 3.4 (2014): 69-86.